Periodic surface structures on Ni–Fe film induced by a single femtosecond laser pulse with diffraction rings

Kan Zhou (周 侃)[1], **Xin Jia** (贾 鑫)[1,2], **Huixia Xi** (郗慧霞)[1], **Jukun Liu** (刘聚坤)[1],
Donghai Feng (冯东海)[1], **Shian Zhang** (张诗按)[1], **Zhenrong Sun** (孙真荣)[1],
and **Tianqing Jia** (贾天卿)[1,*]

[1]*State Key Laboratory of Precision Spectroscopy, East China Normal University, Shanghai 200062, China*
[2]*Department of Mathematics and Physics, Shanghai Dianji University, Shanghai 201306, China*
*Corresponding author: tqjia@phy.ecnu.edu.cn
Received October 24, 2016; accepted December 15, 2016; posted online January 16, 2017

This Letter reports the formation of periodic surface structures on Ni–Fe film irradiated by a single femtosecond laser pulse. A concave lens with a focus length of −150 mm is placed in front of an objective (100×, NA = 0.9), which transforms the Gaussian laser field into a ring distribution by the Fresnel diffraction. Periodic ripples form on the ablation area after the irradiation of a single femtosecond laser pulse, which depends on the laser polarization and laser fluence. We propose that the ring structure of the laser field leads to a similar transient distribution of the permittivity on the sample surface, which further launches the surface plasmon polaritons. The interaction of the incident laser with surface plasmon polaritons dominates the formation of periodic surface structures.

OCIS codes: 220.4241, 160.3900, 240.6700, 320.7090.
doi: 10.3788/COL201715.022201.

Laser-induced periodic surface structures (LIPSSs) have been studied intensely in the last five decades[1–8]. Initial reports on the formation of LIPSSs were usually irradiated by a continuous wave (CW) or long duration laser pulses [nanosecond (ns) laser]. The periods of these structures (are usually ripples) were approximately equal to the laser wavelength. These periodic ripples were attributed to the interference between the incident laser and the scattered light caused by surface defects[1–4].

Low spatial frequent LIPSSs (LSFL) have been observed in semiconductors, dielectrics, and metals after the irradiation of femtosecond (fs) laser pulses[7–27]. Laser polarization, fluence, and the number of laser pulses have been identified as the key parameters for the LSFL formation. Experimental results indicated that the dynamics of a fs laser-induced LSFL were rather different from the near-wavelength ripples induced by a CW and a ns laser. For a normal incident laser with a wavelength λ, the ripple periods changed in the range of 0.5λ–0.95λ[15]. They increased with the increase of the laser fluences and decreased with the increase of the laser pulse numbers[16]. The classical scattering model, which was used to explain the LIPSSs formation irradiated by long duration laser pulses, was too simple to explain the formation of a fs laser-induced LSFL. In order to explain the formation mechanism, several explanations have been proposed, such as the interference between the laser field and surface plasmon polaritons (SPPs), interference between laser and scattered light, self-organization, and coulomb explosion[8–17]. However, it is still difficult to evaluate which mechanism contributes mainly to the LSFL formation under the irradiation of fs laser pulses. After each pulse radiation, ablation craters, surface debris, and LSFL on

the surface will enhance the scattered light and surface plasmons, and further influence the formation of LSFL irradiated by the subsequent laser pulses[18,19]. The myriad of changes of the LSFL phenomena are rather difficult to be fully explained by any one of these scenarios. The formation mechanism of fs laser-induced LSFL is still an open problem.

Single-pulse irradiation can provide fundamental information of fs laser–matter interaction, which is important for investigating the origin of an LSFL[18–20]. Murphy *et al.* fabricated Au micro-disks 110 nm thick on Si substrates, and studied the formation of periodic ripples near the Au–Si edges after irradiation of a single fs laser pulse. By changing the laser polarization orientation, they found that the LSFL formation was dominated by SPPs excitation or by Fresnel diffraction[18,19]. Yang *et al.* studied the generation and erasure of periodic ripples on nanoparticle-covered silicon induced by a single fs pulse with a different laser fluence, and found that these phenomena were due to the competition between periodic surface structuring originated from the interference of the laser field and SPPs and surface smoothing associated with surface melting[20].

The above references focused on the mechanisms of the LSFL formation on semiconductors by using the surface micro/nanostructures as defects after the irradiation of a single pulse. In this Letter, we report the formation of periodic ripples on a smooth surface of Ni–Fe film after irradiation by a single fs laser pulse with diffraction rings. The experiments were performed in a microscope (Nikon, 80i) with an objective (100×, NA = 0.9). A concave lens was put in front of the objective, which introduced several ring structures on the laser field by Fresnel diffraction. Recently, transient reflectivity and dielectric function

of metal and semiconductors were studied experimentally and theoretically[28,29]. The transient variation of optical properties was proposed to greatly influence the formation of LIPSSs[17]. In this Letter, "transient permittivity" is used to present the transient variation of optical properties of Ni. The surface electron density affected the interface permittivity between the surface and the environment[9–11]. When the electron density depends on laser fluence, the permittivity in turn depends on laser fluence. Due to the diffraction, at the area with maxima intensity of the diffraction rings, the transient variation of the permittivity is maxima, which works like surface defects and launches the SPPs. Reference [30] reported on the LSFL formation by single-pulse irradiation because the SPPs can be excited near a groove. Therefore, we propose that the ring laser field leads to a similar distribution of transient permittivity on the sample surface, which further evokes SPPs. The interaction of the incident laser field and SPPs dominates the formation of periodic surface structures.

Our experiments were conducted on a commercial Ti:sapphire regenerative amplifier laser system (Legend Elite, Coherent). It generated a laser at a center wavelength of 800 nm with a pulse duration of 50 fs. The laser system operated at a repetition rate of 100 Hz, and a single laser pulse was selected by an electronic shutter. The laser beam was entered in a microscope (Nikon, 80i), in which an objective (100×, NA = 0.9) was used to focus the laser on the sample surface, as shown in Fig. 1. In order to legibly image the surface structures, the sample was moved to an object plane. However, the object plane was very close to the focus plane. The laser spot with a diameter of 1.5 μm was too small to obtain enough periodic ripples. Therefore, a concave lens with a focus length of −150 mm was placed at 120 mm in front of the objective to expand the pump laser beam. The laser spot on the object plane was extended to 28 μm in diameter with several diffraction rings in the laser field, as shown in the inset of Fig. 1[13]. The image of the laser field was obtained by measuring the emission from a ZnSe crystal surface. In the experiments, the focus length of the concave lens was very important.
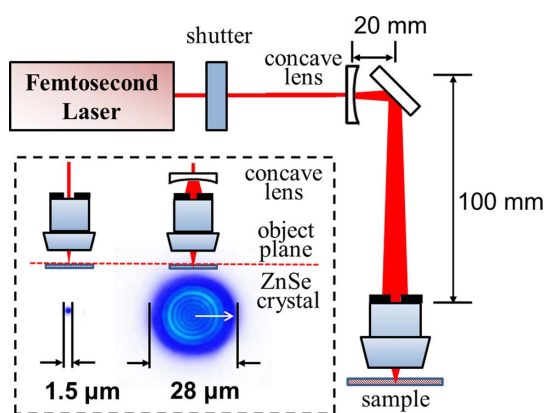

Fig. 1. Sketch of the experimental setup. Inset: the laser field on the object plane with and without the concave lens, respectively.

If the focus length was too long, the diffraction effect was rather weak. However, if the focus length was too short, most of the laser energy was blocked out of the objective, and the sample could not be ablated by one laser pulse. The laser energy on the sample surface was directly measured by a laser energy sensor (PE9-C, OPHIR). The detector with a diameter of 10 mm was placed 3 mm below the objective, where the laser beam was expanded to a diameter of 5 mm. In this Letter, the laser fluence is calculated by taking the focus spot with a diameter of 28 μm, as shown in the inset in Fig. 1.

The sample used in the experiment was a Ni–Fe alloy film deposited on a silica substrate by magnetron sputtering. The main composition of the Ni–Fe alloy was 80% Ni and 20% Fe. The deposition rate was 13 nm/min for 30 min, and the film was 400 nm thick. The magnetic properties of $Ni_{80}Fe_{20}$ "Permalloy" thin films have been studied extensively for the ubiquitous use in integrated magnetic devices[31]. Structures on the $Ni_{80}Fe_{20}$ film, such as stripes, are produced as a magnetoresistive sensor[32]. The sample was mounted on an XYZ translation stage with a resolution of 1 μm. After laser irradiation, the ablation areas were measured by an atomic force microscope (AFM, Nanonavi E-Sweep, NSK).

Figure 2(a) shows the AFM micrographs of an ablated spot after irradiation by a single, linearly polarized laser pulse at a fluence of 0.90 J/cm². There are several circular ring structures formed on the sample surface. The height trace along the arrow perpendicular to the laser polarization is shown as the dot curve in Fig. 2(b). The overall ablation depth is about 10 nm, and the groove depth is about 5 nm. Owing to the concave lens, the laser field is no longer a Gaussian distribution but circular rings following the Huygens–Fresnel principle. The intensity distribution along the arrow in the inset in Fig. 1 is also shown as the solid blue curve in Fig. 2(b), which is obtained by measuring the emission from a ZnSe crystal surface. It fits well with the dot curve of height trace, which indicates that these ablation rings are caused by light diffraction and are called light diffraction-induced ablation rings (LDIARs).

The height trace of the structures along the arrow parallel to the laser polarization in Fig. 2(a) is shown in Fig. 2(c). Similar to the height trace in Fig. 2(b), there are several LDIARs agreeing well with the ring distribution of the laser field. However, the LDIARs depths are much deeper, about 20 nm. Besides the LDIARs, there are two kinds of ripples that are perpendicular to the laser polarization formed on the ablation spot. One kind comes from the split of LDIARs. Four LDIARs close to the spot center are all split into two ripples. The widths of these ripples change in the range of 400–700 nm, which depend on the LDIAR's width. The fifth LDIAR is split into three ripples with a space of 600 nm. Two ripples are observed in the groove at the outer edge of the fifth LDIAR. The ripple depths are of 4–10 nm. The other kind of ripples is at the outer side of the fifth LDIAR. Three ripples with a space of 460 nm formed there, and the outward ripples become
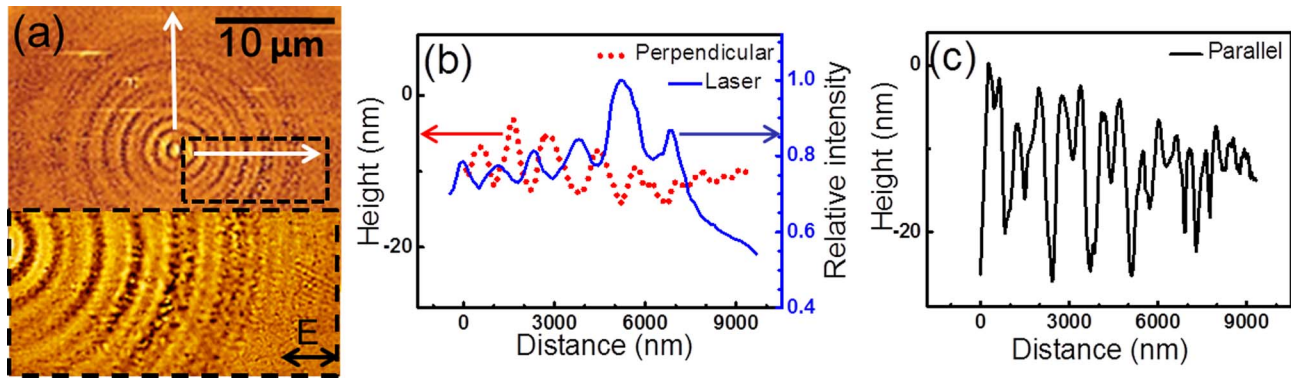
Fig. 2. (a) AFM micrographs of the ablated spot after irradiation by a single laser pulse at a fluence of 0.90 J/cm². The illustration shows the magnified details of the marked region. The black arrow shows the polarization E of the incident laser. (b) The height trace along the arrow perpendicular to the laser polarization, and (c) parallel to the laser polarization.

shallow. There is no confinement from the diffraction ring, and the ripple widths agree well with the results reported in Refs. [9–12].

The ultrafast dynamics of fs laser ablation in metals, such as electron excitation, electron–phonon coupling, electron heating and thermal conductivity, etc., have been studied intensely[33,34]. The Fermi level cuts through the d band in Ni, resulting in a very high density of electron states at the Fermi level[34]. The laser excitation affects the evolution of the density of d states, and the chemical potential and optical properties evolve significantly, including the air–metal interface permittivity[29]. The electron excitation takes place in 1 fs, which makes the permittivity distribution change simultaneously with the irradiation of the fs laser pulse. The transient modulated permittivity lasts for hundreds of fs to picoseconds (ps)[35,36]. At the area with maxima intensity of the diffraction rings, the transient variation of the permittivity is maxima, which works like surface defects and launches SPPs[37–40]. The interference of the laser field and SPPs modulates the laser field, and further causes a modulated energy deposition. The two kinds of ripples both originate from the interaction of the laser field and the SPPs.

Many experimental and theoretical studies indicated that the SPP's excitation would evoke redistribution of the light field on a metal surface, which depended on the light wavelength, permittivity, and surface structures[37–40]. The interaction between the SPPs and the laser field induces the localization of laser field on the peak and valley of the LDIARs, and further stimulates the LDIARs to split into fine ripples[8,12]. Therefore, the ripple widths depend on the LDIAR's widths. The widths of the four inner LDIARs are 850, 1500, 1350, and 1400 nm, and the widths of ripples originated from their splitting are 430, 720, 630, and 700 nm, respectively.

The other kind of ripples is caused by the propagating SPPs at the outer side of the diffraction rings. There is no diffraction ring that confines the SPP's spreading[38–40], and the ripple widths are nearly equal to the SPP's wavelength[9–20].

In Fig. 2(a), the ripples are not as clear as the LDIARs. For the ripples induced by a single fs laser pulse, the production of surface plasma, the excitation of the SPPs, the modulation of the laser field, and the periodic energy deposition, all of these processes have to be finished within the duration of the laser pulse irradiation. The ripples are usually very shallow[41], and the AFM images are not clear.

In order to study the role of the diffraction rings of the laser field in the SPP's excitation and ripples formation, we conducted experiments to study the formation of periodic ripples irradiated by a single Gaussian laser pulse. Because there are no diffraction rings, the SPPs cannot be excited by a single laser pulse. Therefore, no matter how intense the laser power is, no periodic ripples are formed on the sample surface. These results indicate that the formation of periodic ripples is closely related to the diffraction rings in the laser field.

In order to further confirm that the ripples originated from the SPP's excitation, we rotated the laser polarization and found that the ripples rotated synchronously. The ripples are nearly perpendicular to the polarization of incident laser, as shown in Fig. 3, which agrees well with the mechanism that the ripples are caused by the interaction of the laser field and the SPPs.

Because of the diffraction effects of the concave lens, there are several diffraction rings in the laser field at the object plane, as shown in Fig. 1. In this case, the wavefront
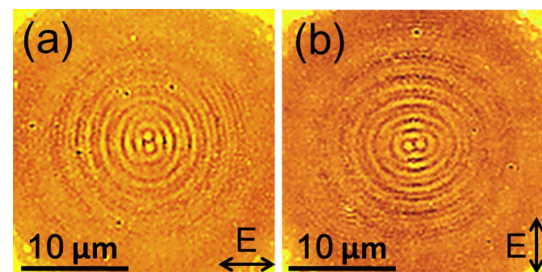

Fig. 3. AFM micrograph of the ablated spot after irradiation by a single laser pulse with (a) horizontal polarization and (b) vertical polarization.

or the polarization will change correspondingly[38]. We simulate the propagating field using the finite element method (COMSOL) adopting adaptive mesh[42]. The results indicate that there are several diffraction maxima at the focus plane, where the laser polarization direction rotates in a small range of $-10° - +10°$. Therefore, the ripples are nearly perpendicular to the polarization of the incident laser.

In order to legibly image the surface structures, the sample was moved to the object plane, which was close to the focus plane. In this case, the laser focus will split into two lobes perpendicular to the laser polarization[38–40]. In our experiments, the sample surface can be observed clearly in a range of $-10 - +10$ μm, hence, in some cases there is one circle, and in others there are two circles next to each other in the center of the ablation spot, as shown in the AFM images in Figs. 2(a) and 3.

Figures 4(a) and 4(b) show the AFM micrographs of the ablated spots after irradiation by a single laser pulse at fluences of 1.67 and 0.76 J/cm², respectively. The height traces along the arrows are shown in Fig. 4(c). For the laser fluence of 1.67 J/cm², the film is greatly ablated with many particles to adhere on. Energy dispersive spectroscopy measured by a scanning electron microscope revealed that the nanoparticles were oxide[43]. These particles greatly disturb the measurement of the ablation spot. Compared with Fig. 2(c), the ablation depth becomes deeper with an increasing laser fluence, but the morphologies of the two spots are similar. The LDIARs split, and the induced ripples are both observed. Hashida *et al.* studied the laser fluence dependence of periodic ripples formed on metal surfaces and found that the formation of periodic ripples depended not only on metal properties, but also on the electron density of surface plasma
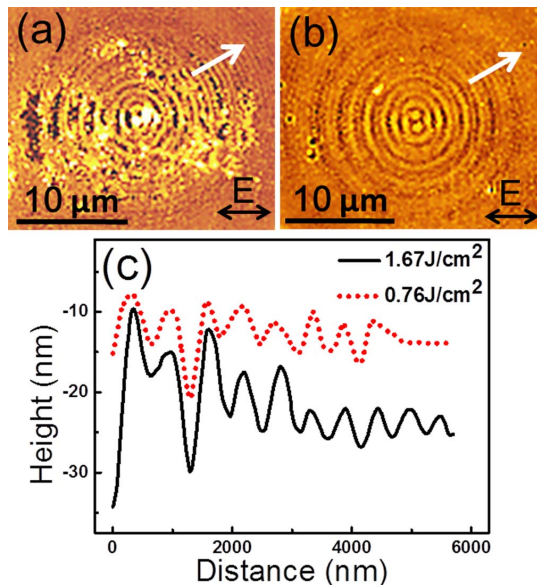

Fig. 4. AFM micrograph of the ablation spot after irradiation by a single laser pulse at fluences of (a) 1.67 and (b) 0.76 J/cm². (c) The height traces along the arrows shown in (a) and (b).
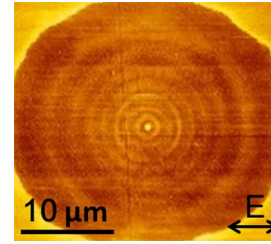

Fig. 5. AFM micrograph of the ablated spot after irradiation by a single laser pulse at a fluence of 0.63 J/cm².

produced by fs laser pulses[9–11]. When increasing the laser fluence, the surface electron density and the SPP's wavelength become larger, resulting in wider periodic ripples. Figure 4(c) shows that the outside ripples are with a space of 530 nm for the fluence of 1.67 J/cm², which is bigger than the ripples for the fluence of 0.90 J/cm². This phenomenon agrees well the mechanism that the ripples originate from the SPP's excitation.

By decreasing the laser fluence to 0.76 J/cm², as shown in Fig. 4(b), the LDIARs' depths are very shallow, less than 10 nm. Even more, the outer three ripples are not observed. The SPPs originated from the diffraction maxima propagate mainly in two directions parallel to the laser polarization. These SPPs interact with each other and enhance the SPPs intensity. Therefore, the ripples between the diffraction rings are deeper than those in the outer side of the LDIARs[40].

Figure 5 shows the AFM micrograph of the ablation spot after irradiation by a single laser pulse at a fluence of 0.63 J/cm². Several LDIARs formed in the ablation spot, which fit well with the ring structures of the laser field. However, no ripples or LDIAR splits are found in any direction. The contrast ratio of the transient permittivity at the diffraction rings greatly affects the SPP's excitation. When the laser intensity is insufficient, the modulation of the transient permittivity is rather weak, or the formation process of the transient modulated permittivity lasts so long that the periodic deposition of the laser energy cannot take place in time within the laser pulse duration. Hence, there are no ripples produced, only the LDIARs formed on the sample surface. The result agrees well with the mechanism that the transient modulated permittivity launches the SPPs and further induces the formation of ripples.

In conclusion, periodic surface structures are observed on Ni–Fe film after the irradiation of a single fs laser pulse with diffraction rings. The ring laser field leads to a similar distribution of transient permittivity on the sample surface and evokes the excitation of SPPs. The interaction of the fs laser with the SPPs dominates the formation of periodic surface structures.

References and notes

1. M. Birnbaum, J. Appl. Phys. **36**, 3688 (1965).
2. D. C. Emmony, R. P. Howson, and L. J. Willis, Appl. Phys. Lett. **23**, 598 (1973).
3. P. M. Fauchet and A. E. Siegman, Appl. Phys. Lett. **40**, 824 (1982).
4. J. E. Sipe, J. F. Young, J. S. Preston, and H. M. Driel, Phys. Rev. B **27**, 1141 (1983).
5. Y. Shimotsuma, P. G. Kazansky, J. R. Qiu, and K. Hirao, Phys. Rev. Lett. **91**, 247405 (2003).
6. T. Q. Jia, H. X. Chen, M. Huang, F. L. Zhao, J. R. Qiu, R. X. Li, Z. Z. Xu, X. K. He, and H. Kuroda, Phys. Rev. B **72**, 125429 (2005).
7. X. Jia, T. Q. Jia, Y. Zhang, P. X. Xiong, D. H. Feng, Z. R. Sun, J. R. Qiu, and Z. Z. Xu, Opt. Lett. **35**, 1248 (2010).
8. A. Y. Vorobyev and C. L. Guo, Laser Photon. Rev. **7**, 385 (2013).
9. S. Sakabe, M. Hashida, S. Tokita, S. Namba, and K. Okamuro, Phys. Rev. B **79**, 033409 (2009).
10. K. Okamuro, M. Hashida, Y. Miyasaka, Y. Ikuta, S. Tokita, and S. Sakabe, Phys. Rev. B **82**, 165417 (2010).
11. M. Hashida, Y. Ikuta, Y. Miyasaka, S. Tokita, and S. Sakabe, Appl. Phys. Lett. **102**, 174106 (2013).
12. S. S. Hou, Y. Y. Huo, P. X. Xiong, Y. Zhang, S. A. Zhang, T. Q. Jia, Z. R. Sun, J. R. Qiu, and Z. Z. Xu, J. Phys. D: Appl. Phys. **44**, 505401 (2011).
13. X. Jia, T. Q. Jia, N. N. Peng, D. H. Feng, S. A. Zhang, and Z. R. Sun, J. Appl. Phys. **115**, 143102 (2014).
14. A. Y. Vorobyev, V. S. Makin, and C. L. Guo, J. Appl. Phys. **101**, 034903 (2007).
15. M. Huang, F. L. Zhao, Y. Cheng, N. S. Xu, and Z. Z. Xu, ACS Nano **3**, 4062 (2009).
16. J. Bonse and J. Kruger, J. Appl. Phys. **108**, 034903 (2010).
17. J. Bonse, A. Rosenfeld, and J. Kruger, J. Appl. Phys. **106**, 104910 (2009).
18. R. D. Murphy, B. Torralva, D. P. Adams, and S. M. Yalisove, Appl. Phys. Lett. **102**, 211101 (2013).
19. R. D. Murphy, B. Torralva, D. P. Adams, and S. M. Yalisove, Appl. Phys. Lett. **104**, 231117 (2014).
20. M. Yang, Q. Wu, Z. D. Chen, B. Zhang, B. Q. Tang, J. H. Yao, I. D. Olenik, and J. J. Xu, Opt. Lett. **39**, 343 (2014).
21. X. Jia, Y. Yuan, D. Yang, T. Jia, and Z. Sun, Chin. Opt. Lett. **12**, 113203 (2014).
22. Y. Yang, J. Yang, C. Liang, H. Wang, X. Zhu, D. Kuang, and Y. Yang, Appl. Phys. A **92**, 635 (2008).
23. Y. Yuan and J. Chen, Chin. Opt. Lett. **14**, 011404 (2016).
24. Y. Yang, J. Yang, C. Liang, and H. Wang, Opt. Express **16**, 11259 (2008).
25. F. Meng, J. Hu, W. Han, P. Liu, and Q. Wang, Chin. Opt. Lett. **13**, 062201 (2015).
26. Z. Cui, Y. Li, W. Wang, C. Lin, and B. Xu, Chin. Opt. Lett. **13**, 011402 (2015).
27. K. Mishchik, G. Cheng, G. Huo, I. M. Burakov, C. Mauclair, A. Mermillod-Blondin, A. Rosenfeld, Y. Ouerdane, A. Boukenter, O. Parriaux, and R. Stoian, Opt. Express **18**, 24809 (2010).
28. A. J. Sabbah and D. M. Riffe, Phys. Rev. B **66**, 165217 (2002).
29. J. P. Colombier, F. Garrelie, N. Faure, S. Reynaud, M. Bounhalli, E. Audouard, R. Stoian, and F. Pigeon, J. Appl. Phys. **111**, 024902 (2012).
30. K. R. P. Kafka, D. R. Austin, H. Li, A. Y. Yi, J. Cheng, and E. A. Chowdhury, Opt. Express **23**, 19432 (2015).
31. R. Jhrome, T. Valet, and P. Galtier, IEEE Trans. Mag. **30**, 4878 (1994).
32. D. J. Mapps, Y. Q. Ma, and M. A. Akhter, Sens. Actuators **81**, 60 (2000).
33. V. Schmidt, W. Husinsky, and G. Betz, Phys. Rev. Lett. **85**, 3516 (2000).
34. Z. B. Lin and L. V. Zhigilei, Appl. Surf. Sci. **253**, 6295 (2007).
35. L. P. Shi, W. X. Li, Y. D. Wang, X. Lu, L. E. Ding, and H. P. Zeng, Phys. Rev. Lett. **107**, 095004 (2011).
36. T. Schneider, D. Wolfframm, R. Mitzner, and J. Reif, Appl. Surf. Sci. **154**, 565 (2000).
37. K. F. MacDonald, Z. L. Samson, M. I. Stockman, and N. I. Zheludev, Nat. Photon. **3**, 55 (2009).
38. A. Bouhelier, F. Ignatovich, A. Bruyant, C. Huang, G. C. Francs, J. C. Weeber, A. Dereux, G. P. Wiederrecht, and L. Novotny, Opt. Lett. **32**, 2535 (2007).
39. H. W. Gao, J. Henzie, and T. W. Odom, Nano Lett. **6**, 2104 (2006).
40. F. D. Stefani, K. Vasilev, N. Bocchio, N. Stoyanova, and M. Kreiter, Phys. Rev. Lett. **94**, 023005 (2005).
41. F. Garrelie, J. P. Colombier, F. Pigeon, S. Tonchev, N. Faure, M. Bounhalli, S. Reynaud, and O. Parriaux, Opt. Express **19**, 9035 (2011).
42. Y. Y. Huo, T. Q. Jia, Y. Zhang, H. Zhao, S. A. Zhang, D. H. Feng, and Z. R. Sun, Appl. Phys. Lett. **104**, 113104 (2014).
43. C. A. Zuhlke, T. P. Anderson, and D. R. Alexander, Appl. Phys. Lett. **103**, 121603 (2013).